ACCSCIENCE PUBLISHING

Global Translational Medicine

ORIGINAL RESEARCH ARTICLE

Channel reduction in AdaBoost ensemble models for energy-efficient ambulatory seizure detection

Aangi Shah and Milan Toma*

Algorithmic Medicine Laboratory, Department of Osteopathic Manipulative Medicine, College of Osteopathic Medicine, New York Institute of Technology, Old Westbury, New York, United States of America

Abstract

Wearable electroencephalogram (EEG) devices offer promising solutions for continuous seizure monitoring in out-of-hospital settings. However, the adoption of medical-grade wearable devices remains limited by the power consumption demands of edge computing, where each active EEG channel contributes to energy expenditure through signal processing and feature extraction operations. Optimizing algorithms through feature reduction may extend battery life without compromising diagnostic reliability. This study evaluated a feature reduction strategy for a 100-tree AdaBoost ensemble model applied to binary seizure detection using the Bangalore EEG Epilepsy Dataset, comprising recordings from 60 subjects. A patient-aware data partitioning scheme (70/15/15 split) was implemented to ensure complete separation of patient identities across training, validation, and testing subsets. Feature importance scores were extracted from the trained ensemble to identify less discriminative EEG channels, and classification performance was compared between a baseline 16-channel configuration and a reduced 12-channel configuration following removal of the four least important channels. The baseline 16-channel model achieved 97.56% test accuracy, 97.29% sensitivity, 98.50% specificity, and a 2.71% seizure miss rate. Following the removal of channels x_5, x_9, x_{11}, and x_{13}, the reduced 12-channel model achieved 97.11% test accuracy, 96.71% sensitivity, 98.50% specificity, and a 3.29% seizure miss rate. The 25% reduction in active channels resulted in only a 0.45 percentage-point decrease in accuracy while yielding an estimated 33.33% theoretical extension in battery operating duration. Strategic channel reduction based on feature importance analysis can improve computational efficiency while maintaining comparable seizure detection performance. These findings support the development of energy-efficient, long-term ambulatory EEG monitoring devices that balance diagnostic reliability with extended operational duration.

Keywords: Seizure detection; AdaBoost ensemble; Electroencephalogram; Feature reduction; Wearable devices; Machine learning

***Corresponding author:**
Milan Toma
(tomamil@tomamil.com)

Citation: Shah A, Toma M. Channel reduction in AdaBoost ensemble models for energy-efficient ambulatory seizure detection. *Global Transl Med*. doi: 10.36922/GTM026220022

Received: May 26, 2026

Revised: June 30, 2026

Accepted: July 10, 2026

Published online: July 30, 2026

1. Introduction

Epilepsy is a chronic neurological condition characterized by recurrent unprovoked seizures, affecting approximately 50 million individuals worldwide, with 80% residing

in low- and middle-income countries.[1,2] Seizures manifest heterogeneously, ranging from brief episodes of impaired awareness to loss of consciousness.[3] Clinically, seizures are categorized as generalized onset (rapidly engaging bilateral brain networks) or focal onset (originating within one hemisphere), with focal seizures sometimes spreading bilaterally as secondarily generalized tonic-clonic seizures.[4,5]

Electroencephalogram (EEG) testing remains a key diagnostic tool for epilepsy, with contemporary criteria permitting diagnosis when recurrence probability exceeds 60% following a single event.[6] EEG also serves to characterize antiseizure medication efficacy.[7] However, traditional hospital-based monitoring faces substantial limitations: standard 20–30-minute examinations frequently fail to capture interictal epileptiform activity, while extended video-EEG monitoring requires inpatient admission for periods typically limited to several days.[6,8,9]

Hospital-based facilities are often geographically inaccessible and restrict patients from daily activities, failing to capture real-world seizure triggers.[10,11] Manual review of high-density recordings is time-consuming and susceptible to inter-observer variability.[8,12] Furthermore, the psychological burden of tethered monitoring equipment reduces normal patient activity, creating diagnostic blind spots.

To address these limitations, wearable EEG devices have been developed to enable continuous monitoring in out-of-hospital settings.[13,14] Despite advances in hardware sensor technology, medical-grade wearable adoption remains restricted by the power bottleneck of edge computing, where local data processing results in high energy consumption.[15,16] Each active EEG channel imposes computational demands associated with memory allocation, signal processing, and real-time feature extraction[17], leading to shortened battery life and increased thermal burden that negatively impact patient compliance.[11,14]

Various machine learning approaches have been applied to automated seizure detection in wearable contexts. Deep learning architectures, including convolutional neural networks and recurrent neural networks, have demonstrated high classification accuracy but require substantial computational resources incompatible with power-constrained devices.[18] Support vector machines and random forests have been explored as lower-complexity alternatives, though performance often depends on extensive feature engineering.[19] Ensemble methods such as Adaptive Boosting (AdaBoost) offer a balance between classification performance and computational efficiency by combining weak learners into robust classifiers.[19,20] However, many existing approaches utilize full electrode montages without systematic evaluation of channel reduction strategies to optimize power consumption.

A critical gap exists in the literature regarding the quantitative relationship between EEG channel reduction and seizure detection performance in the context of wearable device constraints. While spatial redundancy in scalp EEG recordings is well documented[21,22], few studies have rigorously evaluated whether strategic channel elimination can meaningfully reduce energy consumption and potentially extend battery life without clinically significant degradation of diagnostic sensitivity. Addressing this gap requires systematic feature importance analysis to identify less informative channels and patient-aware validation to ensure generalizability.

One potential solution involves optimizing algorithms through feature reduction to function within power-constrained devices without sacrificing seizure detection performance.[17,23] Reducing active electrodes decreases energy consumption for data acquisition and processing while extending operational duration.[13] However, such modifications must be validated to ensure diagnostic capabilities are preserved.

The primary objective of this study is to evaluate a feature reduction strategy for a 100-tree AdaBoost ensemble model applied to seizure detection. Using the Bangalore EEG Epilepsy Dataset (BEED) comprising recordings from 60 subjects[24], a standard 16-channel configuration is compared with a reduced 12-channel configuration to quantify the impact on detection accuracy and seizure miss rates.

Secondary objectives include: (i) identification of EEG channels with the lowest discriminative importance through feature importance analysis[20]; (ii) quantification of the tradeoff between classification performance and computational efficiency; and (iii) estimation of power consumption benefits achievable through channel reduction. Model generalizability is validated through patient-aware data partitioning ensuring complete separation of patient identities across training, validation, and testing subsets.

In summary, this study aims to identify an optimized channel configuration demonstrating a favorable balance between computational efficiency and diagnostic reliability, thereby supporting the development of long-term ambulatory EEG monitoring devices.

2. Materials and methods

2.1. Dataset description

In this study, we employed the BEED dataset, a publicly available collection of EEG recordings obtained from 60 subjects. The dataset comprises EEG signals that have been segmented into 20-second epochs and categorized according to seizure status. Each subject contributed 100 EEG segments, yielding a comprehensive dataset suitable for machine learning analysis. The original labeling scheme classified recordings into three distinct categories: healthy controls (labeled as 0), focal seizures (labeled as 1), and generalized seizures (labeled as 2).

For the purposes of this binary classification task, the labeling structure was transformed such that healthy control recordings were designated as "No-Seizure," while both focal and generalized seizure recordings were consolidated into a single "Yes-Seizure" category. This binarization approach reflects the clinical priority of distinguishing between the presence and absence of seizure activity, regardless of seizure subtype. The input feature space consisted of 16 EEG channels, denoted as x_1–x_{16}.

According to the BEED dataset documentation[24], these channels correspond to different brain regions based on the international 10–20 electrode placement system, with coverage spanning frontal, temporal, parietal, occipital, and central regions. The EEG signals were recorded at a sampling rate of 256 Hz and segmented into 20-second epochs. While the dataset confirms adherence to the 10–20 standard, explicit mappings between the generic channel identifiers (x_1–x_{16}) and standard electrode nomenclature (e.g., Fp1, F7, T3) are not provided, which limits precise neuroanatomical localization of individual channels.

The input features provided to the AdaBoost classifier consisted of the raw amplitude values from each of the 16 EEG channels at each sampled time point within the 20-second epochs. No additional feature extraction (e.g., spectral decomposition or statistical summarization) was performed; the classifier operated directly on the preprocessed EEG channel values as provided in the BEED dataset. The dataset preprocessing, including any filtering or artifact rejection, was performed by the original dataset authors prior to public release.

2.2. Computational framework overview

The algorithmic pipeline was implemented in MATLAB and consisted of five principal stages: (i) data preprocessing and label mapping, (ii) patient-aware data partitioning, (iii) class balancing through undersampling, (iv) ensemble model training using the AdaBoost algorithm, and (v) feature importance calculation for subsequent channel reduction. Figure 1 illustrates the complete computational workflow employed in this study.

2.3. Data preprocessing and label transformation

The raw dataset was imported from a comma-separated values file containing EEG recordings with their corresponding class labels. The preprocessing stage involved filtering the dataset to retain only those records with valid class labels, specifically those entries where the target variable y assumed values within the set {0,1,2}. This filtering operation excluded any corrupted or ambiguously labeled recordings from subsequent analysis.

Following the filtering operation, a label transformation procedure was applied to convert the multiclass classification problem into a binary classification task. Let y_i denote the original label for the i-th observation. The transformed binary label $\tilde{y}_i$ was computed according to the mapping function:

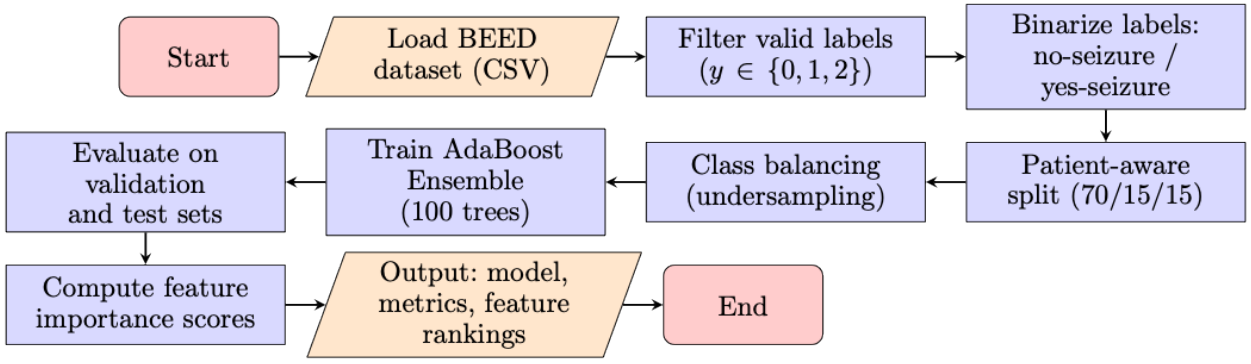

Figure 1. Complete computational workflow for seizure detection using an AdaBoost ensemble model with feature importance-based channel reduction
Abbreviations: BEED: Bangalore Electroencephalogram Epilepsy Dataset; CSV: Comma-separated values.

$$\tilde{y}_i = \begin{cases} \text{"No-Seizure"} & \text{if } y_i = 0 \\ \text{"Yes-Seizure"} & \text{if } y_i \in 1,2 \end{cases} \quad (1)$$

This transformation consolidated focal and generalized seizure events into a unified positive class, thereby framing the detection problem as a dichotomous discrimination between seizure presence and absence. The resulting categorical labels were stored as a new variable appended to the feature matrix, and the original numeric label column was subsequently removed to prevent label leakage during model training.

2.4. Patient-aware data partitioning

A critical consideration in developing generalizable machine learning models for clinical EEG applications is the prevention of information leakage between training and evaluation datasets. When multiple observations originate from the same subject, intra-patient similarities in EEG morphology can artificially inflate performance metrics if observations from the same individual are distributed across both training and testing partitions. To address this concern, a patient-aware data splitting strategy was implemented that ensured complete separation of subject identities across the training, validation, and testing subsets.

The partitioning algorithm operated at the patient level rather than the observation level. Given that each of the N_p = 60 subjects contributed exactly N_r = 100 observations, a patient identification vector was constructed by replicating each patient index across its corresponding observations. Let $P = \{p_1, p_2, \ldots, p_{N_p}\}$ denote the set of unique patient identifiers. The random number generator was initialized with a fixed seed value of 42 to ensure reproducibility, and the patient identifiers were randomly permuted to eliminate any systematic ordering effects.

The permuted patient set was then partitioned according to a 70/15/15 allocation scheme. The number of patients assigned to each subset was determined as follows:

$$N_{\text{train}} = 0.70 \times N_p \quad (2)$$

$$N_{\text{val}} = 0.15 \times N_p \quad (3)$$

$$N_{\text{test}} = N_p - N_{\text{train}} - N_{\text{val}} \quad (4)$$

For the dataset comprising 60 subjects, this allocation resulted in 42 subjects for training, 9 subjects for validation, and 9 subjects for testing. All observations belonging to a given patient were assigned exclusively to one partition, thereby guaranteeing that no patient appeared in multiple subsets. Figure 2 provides a detailed illustration of the patient-aware splitting procedure.

The three-way partitioning strategy (training, validation, and testing) was selected over the two-way splitting strategy (training and testing), which would have required additional validation procedures such as *k*-fold cross-validation, due to methodological considerations. Cross-validation is typically employed when limited data necessitates a two-way split, with the validation set serving dual purposes of hyperparameter tuning and final performance estimation. However, this approach may conflate model selection with model

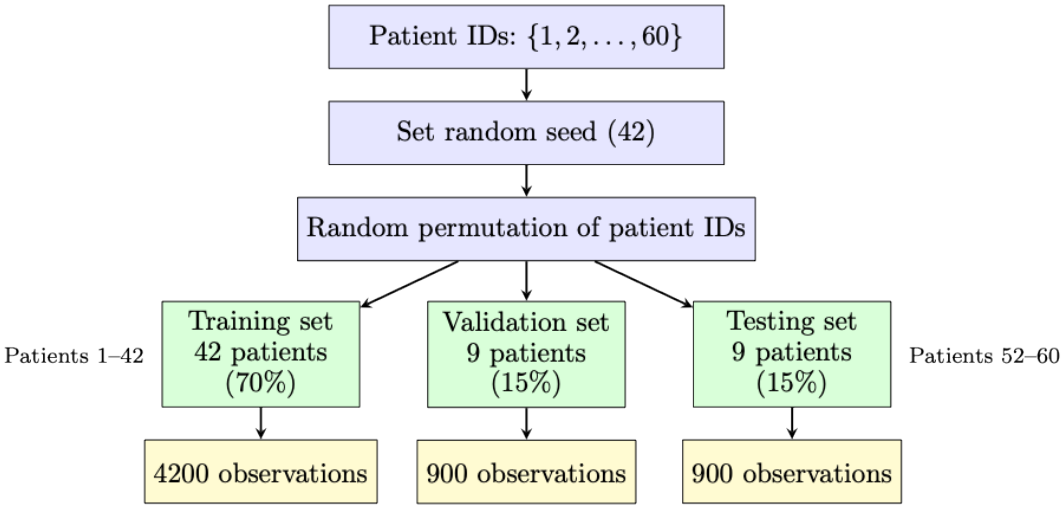

Figure 2. Patient-aware data splitting procedure demonstrating patient-level separation across training, validation, and testing partitions

evaluation, potentially introducing optimistic bias into reported performance metrics. A dedicated three-way split maintains strict separation between the data used for training, hyperparameter selection (validation), and final unbiased evaluation (testing).

2.5. Class balancing through random undersampling

Class imbalance represents a significant challenge in seizure detection tasks, as non-seizure recordings typically outnumber seizure events in clinical datasets. Training machine learning models on imbalanced data can lead to biased classifiers that exhibit poor sensitivity toward the minority class. To mitigate this issue, a random undersampling strategy was applied to the training partition.

The undersampling procedure operated by first identifying the indices of observations belonging to each class within the training set. Let $I_{\text{No}} = \{i : \tilde{y}_i = \text{"No-Seizure"}\}$ and $I_{\text{Yes}} = \{i : \tilde{y}_i = \text{"Yes-Seizure"}\}$ denote the index sets for the negative and positive classes, respectively. The cardinality of the minority class was determined as $n_{\min} = |I_{\text{No}}|$, and an equivalent number of samples was randomly selected from the majority class:

$$I_{\text{Yes}}^{\text{sampled}} \subset I_{\text{Yes}}, \quad \left| I_{\text{Yes}}^{\text{sampled}} \right| = n_{\min} \tag{5}$$

The balanced training set was then constructed by concatenating the complete minority class index set with the randomly sampled majority class indices, followed by a random permutation to shuffle the observation order. This balancing procedure ensured equal representation of both classes during model training, thereby preventing the classifier from developing a bias toward the more prevalent class.

Alternative class balancing strategies such as the Synthetic Minority Over-sampling Technique and cost-sensitive learning through class weights were not evaluated in this study. This decision was deliberate rather than an oversight. The primary objective of the present study was to demonstrate that reducing the number of EEG input channels can preserve classification accuracy while decreasing theoretical power consumption requirements in wearable devices. Achieving this objective required maintaining a simple, interpretable algorithmic pipeline with minimal methodological confounds. Introducing multiple class balancing strategies would have complicated the attribution of any observed performance changes: it would become unclear whether differences between the 16-channel and 12-channel configurations arose from the feature reduction itself or from interactions between the balancing method and the reduced feature space. By adopting random undersampling as a straightforward default approach, the experimental design focused on evaluating channel reduction as the sole manipulated variable, enabling direct interpretation of the efficiency-accuracy tradeoff. Future work investigating optimal class balancing for seizure detection applications may compare multiple strategies, but such comparisons fall outside the scope of the present study.

2.6. AdaBoost ensemble model architecture

The classification model employed in this study was based on the AdaBoost algorithm, a powerful ensemble learning technique that combines multiple weak learners into a strong classifier through iterative reweighting of training samples. The AdaBoost methodology was selected for its computational efficiency, interpretability, and proven effectiveness in binary classification tasks involving biomedical signals.

2.6.1. Theoretical foundation of AdaBoost

The AdaBoost algorithm operates by sequentially training weak classifiers on weighted versions of the training data, where misclassified samples receive increased weights in subsequent iterations. Consider a training set $\{(\mathrm{x}_i, y_i)\}_{i=1}^{N}$ where $\mathrm{x}_i \in \mathbb{R}^{16}$ represents the input feature vector containing 16 EEG channels and $y_i \in \{-1, +1\}$ denotes the binary class label. The algorithm initializes uniform weights for all training samples:

$$w_i^{(1)} = \frac{1}{N}, \; i = 1, 2, \ldots, N \tag{6}$$

At each iteration $t = 1, 2, \ldots, T$, where T denotes the total number of boosting iterations (corresponding to the number of weak learners), the algorithm performs the following steps. First, a weak classifier $h_t(\mathrm{x})$ is trained on the weighted training data to minimize the weighted classification error:

$$\epsilon_t = \sum\nolimits_{i=1}^{N} w_i^{(t)} \cdot \mathbb{I}\left[h_t\left(\mathrm{x}_i\right) \neq y_i\right] \tag{7}$$

where $I[\cdot]$ is the indicator function that returns 1 if the condition is true and 0 otherwise. The contribution coefficient α_t for the weak classifier is then computed based on its classification accuracy:

$$\alpha_t = \frac{1}{2} \ln\left(\frac{1 - \epsilon_t}{\epsilon_t}\right) \tag{8}$$

This formulation assigns larger weights to more accurate classifiers while penalizing those with higher error rates. The sample weights are subsequently updated to emphasize misclassified instances:

$$w_i^{(t+1)} = \frac{w_i^{(t)} \cdot \exp\left(-\alpha_t \cdot y_i \cdot h_t\left(\mathrm{x}_i\right)\right)}{Z_t} \tag{9}$$

where Z_t is a normalization factor ensuring that the weights sum to unity:

$$Z_t = \sum_{i=1}^{N} w_i^{(t)} \cdot \exp\left(-\alpha_t \cdot y_i \cdot h_t\left(\mathrm{x}_i\right)\right) \tag{10}$$

The final ensemble classifier aggregates the predictions of all weak learners through a weighted voting scheme:

$$H\left(\mathrm{x}\right) = \mathrm{sign}\left(\sum_{t=1}^{T} \alpha_t \cdot h_t\left(\mathrm{x}\right)\right) \tag{11}$$

Figure 3 presents a comprehensive visualization of the AdaBoost training procedure.

2.6.2. Model configuration and hyperparameters

The AdaBoost ensemble was configured with $T = 100$ weak learners (decision-tree classifiers), providing sufficient model complexity to capture the discriminative patterns in EEG signals while avoiding excessive computational burden. The selection of 100 estimators was based on preliminary model evaluation and is consistent with commonly used configurations in ensemble learning implementations.

As demonstrated by the learning curves presented in Section 3, classification performance plateaued well before the 100th iteration, suggesting that this value provided adequate model capacity without unnecessary computational overhead. Each weak learner was implemented as a shallow decision tree with a maximum of five splits, constraining the complexity of individual classifiers to ensure that the ensemble learning proceeded gradually rather than achieving immediate saturation. The maximum depth of five splits was chosen to limit individual tree complexity and promote ensemble diversity, consistent with established recommendations for boosted decision tree ensembles in biomedical signal classification.

The learning rate parameter was set to $\eta = 0.1$, which modulates the contribution of each successive weak learner to the ensemble. A reduced learning rate promotes smoother convergence of the training process and helps prevent overfitting by limiting the influence of any single weak classifier. The modified coefficient calculation incorporating the learning rate is expressed as:

$$\tilde{\alpha}_t = \eta \cdot \alpha_t = \frac{\eta}{2} \ln\left(\frac{1-\epsilon_t}{\epsilon_t}\right) \tag{12}$$

The feature matrix for training consisted of the 16 EEG channel values from the balanced training set, denoted as $\mathrm{X}_{\mathrm{train}} \in \mathbb{R}^{N_{\mathrm{bal}} \times 16}$, where N_{bal} represents the number of observations in the balanced training partition. The corresponding label vector $\mathrm{Y}_{\mathrm{train}}$ contained the categorical seizure classifications for each observation.

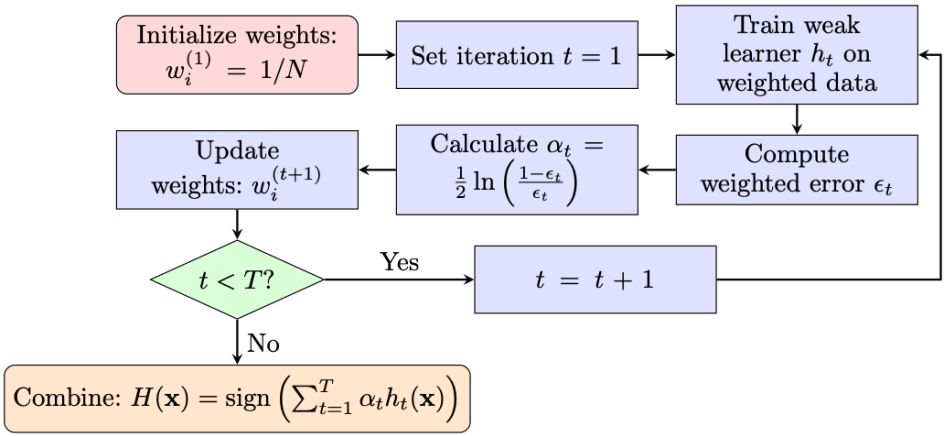

Figure 3. Flowchart illustrating the iterative training procedure of the AdaBoost algorithm, including weight initialization, weak learner training, coefficient calculation, weight updating, and final classifier combination

2.7. Learning curve generation and model evaluation

To assess the training dynamics and generalization performance of the AdaBoost ensemble, learning curves were generated by computing the cumulative classification error at each boosting iteration. The cumulative error measure evaluates the ensemble performance using only the first t weak learners, providing insight into how model accuracy evolves as additional classifiers are incorporated.

For the training set, the cumulative error at iteration t was computed as:

$$E_{\text{train}}^{(t)} = \frac{1}{N_{\text{train}}} \sum_{i=1}^{N_{\text{train}}} \mathbb{I}\left[H^{(t)}(\mathrm{x}_i) \neq y_i \right] \tag{13}$$

where $H^{(t)}(\mathrm{x})$ denotes the ensemble classifier using only the first t weak learners. The corresponding training accuracy at iteration t is given by:

$$A_{\text{train}}^{(t)} = 1 - E_{\text{train}}^{(t)} \tag{14}$$

Similarly, the validation accuracy was computed at each iteration using the held-out validation partition:

$$A_{\text{val}}^{(t)} = 1 - \frac{1}{N_{\text{val}}} \sum_{i=1}^{N_{\text{val}}} \mathbb{I}\left[H^{(t)}\left(\mathbf{x}_i^{\text{val}}\right) \neq y_i^{\text{val}} \right] \tag{15}$$

The divergence between training and validation curves provides diagnostic information regarding potential overfitting, with a widening gap indicating that the model is fitting training-specific patterns that do not generalize well to unseen data.

2.8. Confusion matrix analysis

Model performance was quantified through confusion matrix analysis applied to the training, validation, and testing partitions. For a binary classification problem, the confusion matrix tabulates the counts of true positives (TP), true negatives (TN), false positives (FP), and false negatives (FN). From these quantities, several performance metrics were derived.

The overall classification accuracy measures the proportion of correct predictions:

$$\text{Accuracy} = \frac{\text{TP} + \text{TN}}{\text{TP} + \text{TN} + \text{FP} + \text{FN}} \tag{16}$$

The sensitivity, also known as recall or TP rate, quantifies the model's ability to correctly identify seizure events:

$$\text{Sensitivity} = \frac{\text{TP}}{\text{TP} + \text{FN}} \tag{17}$$

The specificity measures the proportion of non-seizure events correctly classified:

$$\text{Specificity} = \frac{\text{TN}}{\text{TN} + \text{FP}} \tag{18}$$

The seizure miss rate, a clinically relevant metric for wearable device applications, was computed as the complement of sensitivity:

$$\text{Miss rate} = 1 - \text{sensitivity} = \frac{\text{FN}}{\text{TP} + \text{FN}} \tag{19}$$

2.9. Feature importance extraction and channel reduction

A primary objective of this study was to identify opportunities for feature reduction that would decrease computational requirements while preserving seizure detection performance. The AdaBoost ensemble provides intrinsic feature importance scores based on the cumulative contribution of each input variable to the classification decisions across all weak learners.

For decision tree-based weak learners, the importance of feature j is computed by aggregating the weighted impurity decrease across all nodes where feature j is used for splitting:

$$\text{Imp}(j) = \sum_{t=1}^{T} \sum_{n \in \mathcal{N}_t^{(j)}} w_n \cdot \Delta G_n \tag{20}$$

where $\mathcal{N}_t^{(j)}$ denotes the set of nodes in weak learner t that split on feature j, w_n is the weighted proportion of samples reaching node n, and ΔG_n represents the impurity decrease achieved by the split at node n. The impurity decrease for a binary split is calculated using the Gini criterion:

$$\Delta G_n = G_n - \frac{N_L}{N_n} G_L - \frac{N_R}{N_n} G_R \tag{21}$$

where G_n, G_L, and G_R denote the Gini impurity values at the parent node and left and right child nodes, respectively, and N_n, N_L, N_R represent the corresponding sample counts.

The Gini impurity for a node with class distribution p is defined as:

$$G = 1 - \sum_{k=1}^{K} p_k^2 \quad (22)$$

where p_k represents the proportion of samples belonging to class k at the node.

The feature importance scores were extracted from the trained AdaBoost model and sorted in descending order to identify the most influential EEG channels. Figure 4 illustrates the feature ranking and reduction procedure.

2.10. Comparative analysis framework

The experimental design incorporated a comparative analysis between the baseline 16-channel configuration and a reduced 12-channel configuration. The four channels exhibiting the lowest importance scores—specifically channels x_5, x_9, x_{11}, and x_{13}—were identified as candidates for removal based on the feature ranking obtained from the initial model training phase.

A second AdaBoost ensemble was trained using the reduced feature set, maintaining identical hyperparameter settings to ensure a fair comparison. The performance differential between the two configurations was quantified in terms of accuracy degradation, changes in seizure miss rate, and theoretical power consumption reduction. This comparative framework enabled the assessment of the tradeoff between computational efficiency and seizure detection performance, which is critical for deployment in resource-constrained wearable devices.

2.11. Power consumption estimation

The power consumption analysis was based on a theoretical simulation model that accounted for the relationship between active EEG channels and energy expenditure in wearable devices. The computational power required for processing EEG signals scales approximately linearly with the number of active channels, as each channel requires dedicated analog-to-digital conversion, signal conditioning, and feature extraction operations.

Let P_{16} denote the baseline power consumption for the 16-channel configuration. The estimated power consumption for the reduced 12-channel configuration was modeled as:

$$P_{12} = P_{16} \cdot \frac{12}{16} = 0.75 \cdot P_{16} \quad (23)$$

The corresponding improvement in battery life, assuming constant battery capacity C, was estimated as:

$$\Delta T = \frac{C}{P_{12}} - \frac{C}{P_{16}} = \frac{C}{P_{16}}\left(\frac{16}{12} - 1\right) = \frac{C}{P_{16}} \cdot \frac{1}{3} \quad (24)$$

This theoretical framework provided the basis for quantifying the potential operational benefits of feature reduction in terms of extended operational duration for ambulatory monitoring applications.

3. Results

3.1. Baseline 16-channel model configuration

The initial AdaBoost ensemble was trained using the complete set of 16 EEG input channels (x_1–x_{16}) to establish baseline classification performance and to extract feature importance scores for subsequent dimensionality reduction analysis. This baseline configuration served as the reference point against which the reduced-channel

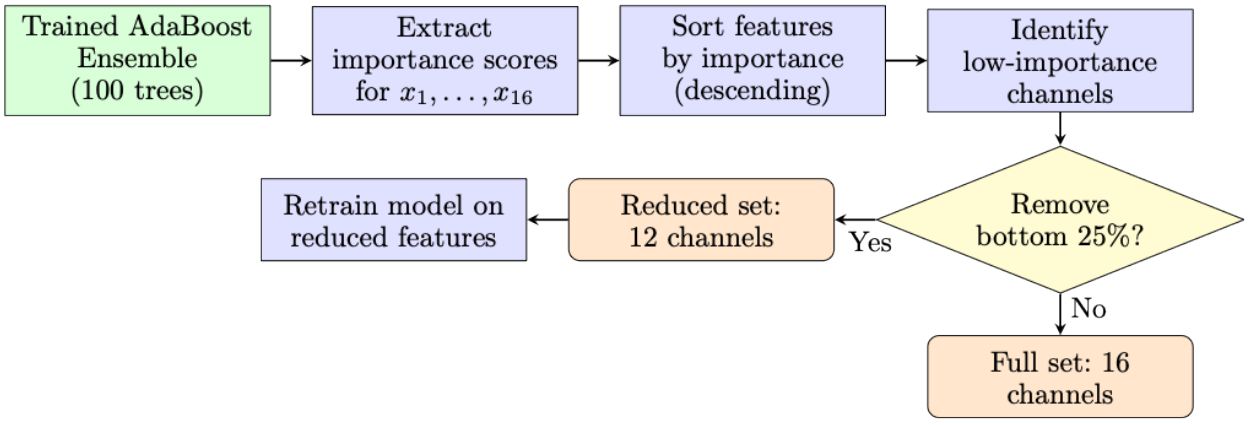

Figure 4. Feature importance extraction and channel reduction workflow illustrating the identification and removal of low-importance electroencephalogram channels based on AdaBoost ensemble feature rankings

model was compared.

3.2. Learning curve analysis for 16-channel configuration

The learning curves depicting the evolution of classification accuracy across boosting iterations for the baseline 16-channel AdaBoost ensemble are presented in Figure 5. The training accuracy exhibited rapid initial improvement, beginning at approximately 97% at the first iteration and approaching 99.9% upon completion of the 100 boosting iterations. The convergence pattern indicates effective learning with minimal overfitting.

The validation accuracy curve demonstrated an increasing trend consistent with effective generalization, commencing at approximately 90% and reaching a plateau of approximately 99% after 60 iterations. The modest gap between training and validation curves indicates that the baseline model achieved strong generalization performance across all 16 input channels.

3.3. Classification performance of 16-channel model

The confusion matrices summarizing the classification outcomes for the training, validation, and testing partitions of the baseline 16-channel model are displayed in Figure 6. Table 1 presents the quantitative performance metrics derived from these confusion matrices.

On the training partition, the baseline model achieved an overall accuracy of 99.96%, with 1,400 TP detections and 1,399 TN classifications. The sensitivity for seizure detection was 100%, with a corresponding seizure miss rate of 0% on the training data.

The validation partition yielded an accuracy of 99.11%, demonstrating robust generalization to unseen patient data. The sensitivity of 98.80% indicated that 494 out of 500 seizure events were correctly detected, with only 6 FN classifications. The specificity of 99.50% confirmed accurate identification of non-seizure episodes.

The testing partition achieved an accuracy of 97.56%

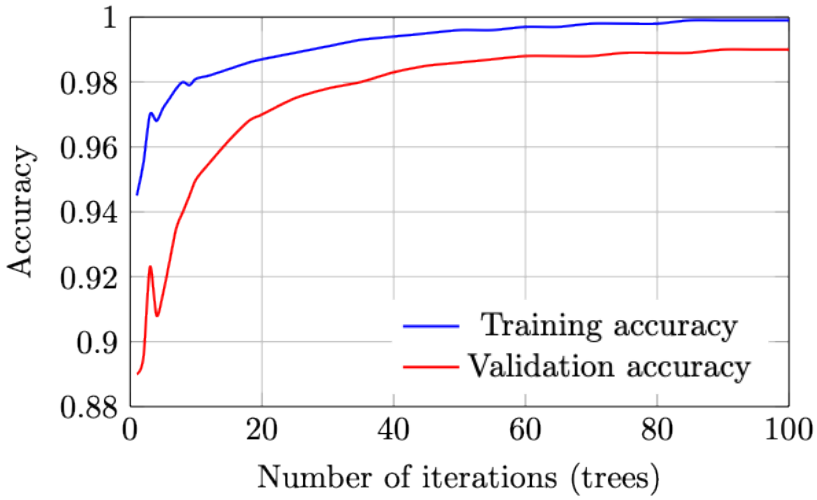

Figure 5. Learning curves showing training and validation accuracy as a function of boosting iterations for the baseline 16-channel AdaBoost ensemble

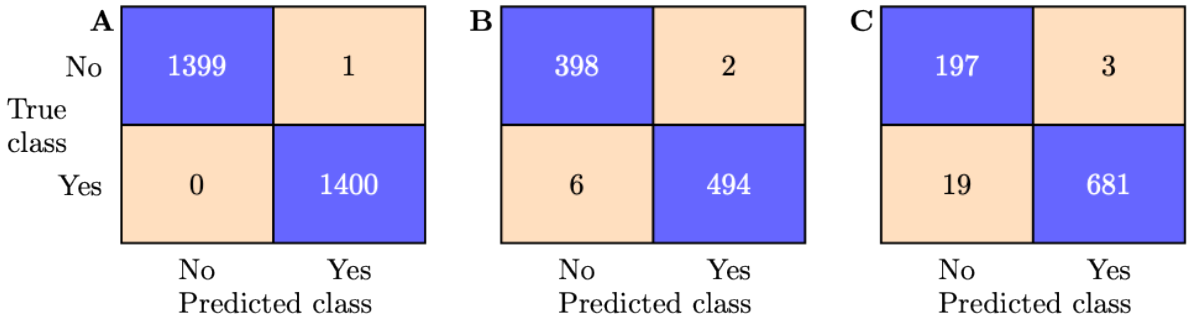

Figure 6. Confusion matrices for the baseline 16-channel AdaBoost ensemble on (A) training, (B) validation, and (C) testing partitions

with a sensitivity of 97.29% and a specificity of 98.50%. The confusion matrix revealed 681 TP detections out of 700 actual seizure events. The seizure miss rate was 2.71%, representing 19 seizure episodes that were incorrectly classified as non-seizure events.

Table 1. Classification performance metrics for the baseline 16-channel AdaBoost ensemble across training, validation, and testing partitions

Metric	Training	Validation	Testing
True negatives	1,399	398	197
False positives	1	2	3
False negatives	0	6	19
True positives	1,400	494	681
Accuracy (%)	99.96	99.11	97.56
Sensitivity (%)	100.00	98.80	97.29
Specificity (%)	99.93	99.50	98.50
Seizure miss rate (%)	0.00	1.20	2.71

3.4. Feature importance distribution in baseline model

The feature importance scores extracted from the trained 16-channel AdaBoost ensemble provided the basis for identifying candidates for channel reduction. To facilitate interpretability and maintain consistency with subsequent analyses, the raw importance scores were normalized by dividing each value by the maximum observed score, thereby scaling the most important feature to a value of unity. Figure 7 presents the normalized and ranked importance values for all 16 input features.

The analysis identified channel x_{16} as the most influential model predictor, achieving a normalized importance score of 1.00, followed closely by channel x_8 with a normalized score of 0.97 and channel x_6 with a normalized score of 0.56. These three channels collectively accounted for a substantial portion of the ensemble's model-derived feature importance.

The complete ranking of the 16 channels in descending order of normalized importance was: x_{16} (1.00), x_8 (0.97), x_6 (0.56), x_{10} (0.43), x_{14} (0.35), x_{15} (0.33), x_3 (0.28), x_4 (0.26), x_2 (0.22), x_{12} (0.22), x_1 (0.12), x_7 (0.12), x_9 (0.04), x_{11} (0.04), x_5 (0.03), and x_{13} (0.01).

The four channels exhibiting the lowest normalized importance scores were identified as x_9 (0.04), x_{11} (0.04), x_5 (0.03), and x_{13} (0.01). These channels collectively contributed less than 1.5% of the total feature importance and were therefore selected as candidates for removal in the subsequent dimensionality reduction analysis.

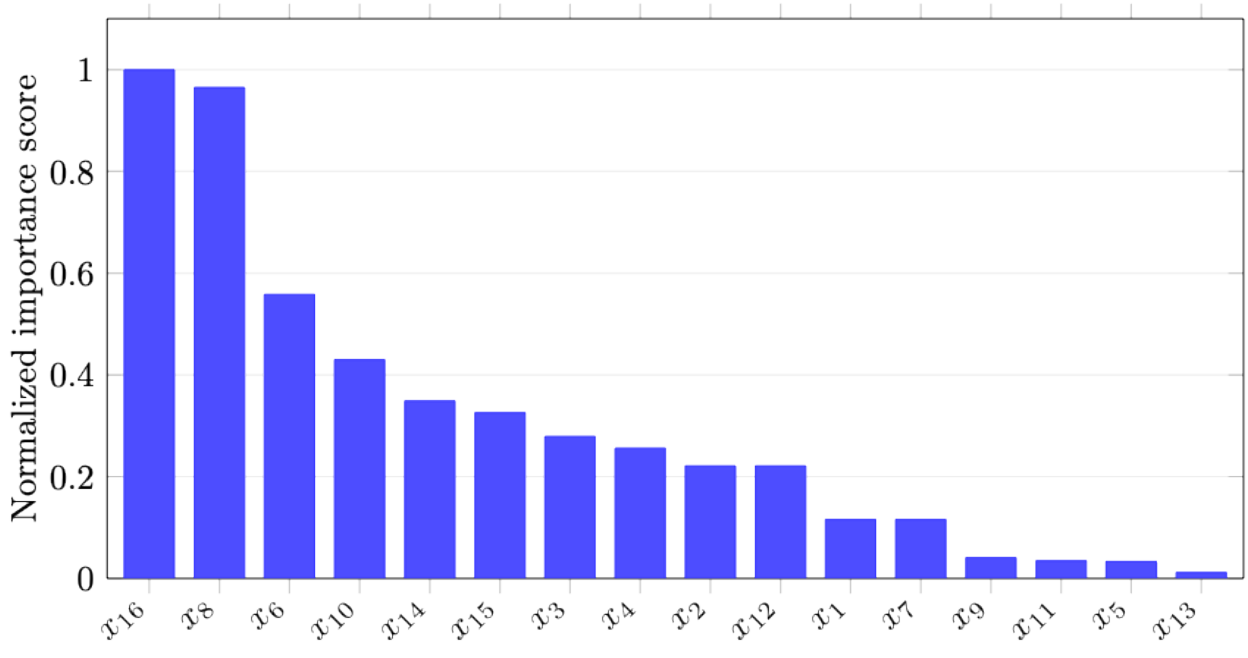

Figure 7. Normalized feature importance scores for the baseline 16-channel configuration, ranked in descending order. Values are scaled relative to the most important channel ($x16 = 1.0$).

3.5. Reduced 12-channel model configuration

Following the feature importance analysis conducted on the baseline 16-channel AdaBoost ensemble, the four EEG channels exhibiting the lowest model-derived importance scores were identified as x_5, x_9, x_{11}, and x_{13}. These channels were subsequently removed from the feature space, yielding a reduced configuration comprising 12 input channels. A second AdaBoost ensemble was trained on this reduced feature set using identical hyperparameter settings to enable direct comparison with the baseline model.

3.6. Learning curve analysis for 12-channel configuration

The learning curves depicting the evolution of classification accuracy across boosting iterations for the reduced 12-channel AdaBoost ensemble are presented in Figure 8. The training accuracy exhibited a characteristic monotonic increase, beginning at approximately 94.5% at the first iteration and reaching 99.9% upon completion of the 100 boosting cycles. The convergence of the training and validation curves indicates stable model performance with limited evidence of overfitting.

The validation accuracy curve demonstrated similar increasing behavior, commencing at approximately 89% and reaching a plateau of approximately 99% after 60 iterations. The gap between training and validation accuracy remained relatively modest throughout the training process, with a maximum divergence of approximately 1 percentage-point observed in the later iterations. This convergence pattern indicates that the reduced model achieved strong generalization performance without exhibiting pronounced overfitting to the training data, despite the removal of four input channels.

3.7. Classification performance of 12-channel model

The confusion matrices summarizing the classification outcomes for the training, validation, and testing partitions of the reduced 12-channel model are shown in Figure 9. Table 2 presents the quantitative performance metrics derived from these confusion matrices.

Table 2. Classification performance metrics for the reduced 12-channel AdaBoost ensemble across training, validation, and testing partitions

Metric	Training	Validation	Testing
True negatives	1,398	398	197
False positives	2	2	3
False negatives	0	7	23
True positives	1,400	493	677
Accuracy (%)	99.93	99.00	97.11
Sensitivity (%)	100.00	98.60	96.71
Specificity (%)	99.86	99.50	98.50
Seizure miss rate (%)	0.00	1.40	3.29

On the training partition, the reduced model achieved an overall accuracy of 99.93%, with 1,400 TP detections and 1,398 TN classifications. The sensitivity for seizure detection was 100%, indicating that the model correctly identified all seizure events within the balanced training

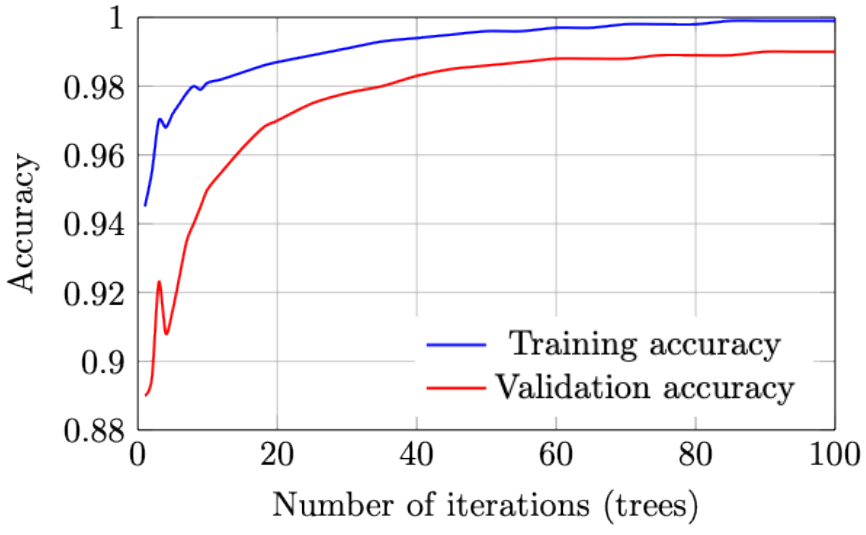

Figure 8. Learning curves showing training and validation accuracy as a function of boosting iterations for the reduced 12-channel AdaBoost ensemble

set. The corresponding seizure miss rate of 0% on the training data reflects the ensemble's complete capture of positive class instances during the learning phase.

The validation partition yielded an accuracy of 99.00%, demonstrating the model's robust ability to generalize to unseen patient data. The sensitivity of 98.60% indicated that 493 out of 500 seizure events were correctly detected, with only 7 FN classifications. The specificity of 99.50% confirmed accurate identification of non-seizure episodes, with merely 2 FP predictions out of 400 negative cases.

The testing partition, which served as the final independent evaluation, achieved an accuracy of 97.11% with a sensitivity of 96.71% and specificity of 98.50%. The confusion matrix revealed 677 TP detections out of 700 actual seizure events, alongside 197 TN classifications out of 200 non-seizure observations. The seizure miss rate was 3.29%, representing 23 seizure episodes that were incorrectly classified as non-seizure events. This metric is of particular clinical significance for wearable monitoring applications, as missed seizure detections could result in delayed intervention.

3.8. Feature importance distribution in reduced model

The feature importance scores extracted from the trained 12-channel AdaBoost ensemble revealed the relative redistribution of model-derived feature contributions following the removal of the four least important predictors. To facilitate interpretability and cross-feature comparison, the raw importance scores were normalized by dividing each value by the maximum observed score, thereby scaling the most important feature to a value of unity. Figure 10 presents the normalized and ranked importance values for all 12 retained input features.

The analysis identified channel x_8 as the most influential model predictor within the reduced feature set, achieving a normalized importance score of 1.00, followed by channel x_{16} with a normalized score of 0.94 and channel x_6 with a normalized score of 0.61. These three channels collectively

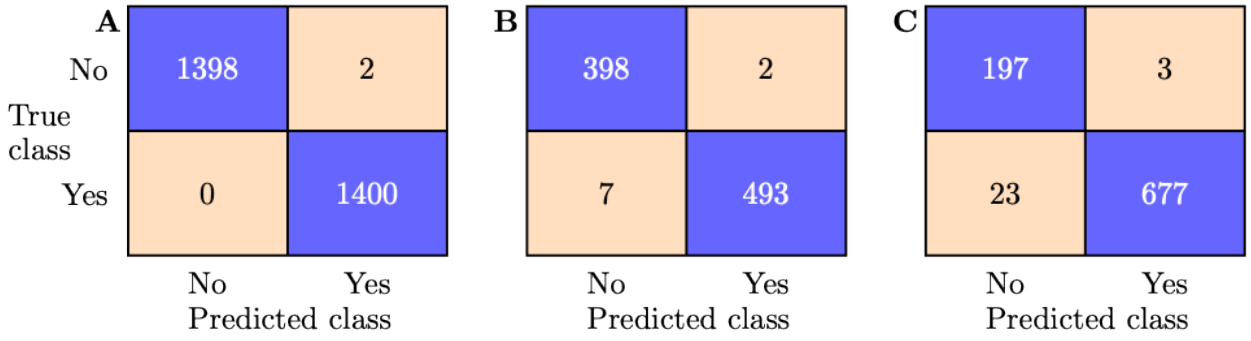

Figure 9. Confusion matrices for the reduced 12-channel AdaBoost ensemble on (A) training, (B) validation, and (C) testing partitions

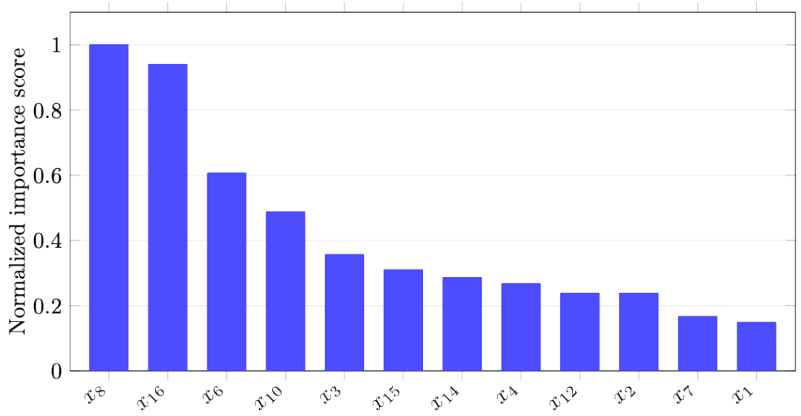

Figure 10. Normalized feature importance scores for the reduced 12-channel configuration, ranked in descending order. Values are scaled relative to the most important channel ($x_8 = 1.0$).

accounted for a substantial portion of the ensemble's model-derived feature importance, with x_8 and x_6 together representing the dominant predictors due to their markedly higher importance relative to the remaining features.

The complete ranking of the 12 retained channels in descending order of normalized importance was: x_8 (1.00), x_{16} (0.94), x_6 (0.61), x_{10} (0.49), x_3 (0.36), x_{15} (0.31), x_{14} (0.29), x_4 (0.27), x_{12} (0.24), x_2 (0.24), x_7 (0.17), and x_1 (0.15). Channels x_7 and x_1 exhibited the lowest normalized importance scores among the retained features, contributing approximately 17% and 15% of the discriminative power of the most important channel, respectively. Despite their relatively lower contributions, these channels were retained as they exceeded the importance thresholds of the removed channels (x_5, x_9, x_{11}, and x_{13}).

3.9. Performance summary and power efficiency implications

The reduced 12-channel AdaBoost ensemble demonstrated competitive classification performance while utilizing 25% fewer EEG channels compared with the baseline configuration. Table 3 summarizes the key performance indicators and estimated efficiency gains.

Table 3. Summary of performance and efficiency metrics for the 12-channel model

Parameter	Value
Number of features	12
Number of boosting iterations	100
Test accuracy (%)	97.11
Test sensitivity (%)	96.71
Test specificity (%)	98.50
Seizure miss rate (%)	3.29
Feature reduction (%)	25.00
Estimated power reduction (%)	25.00
Estimated battery life extension (%)	33.33

According to the power consumption model defined in **Equation 23**, the 25% reduction in active EEG channels corresponds to an estimated 25% decrease in channel-dependent power consumption. Applying **Equation 24**, this channel reduction yields a theoretical 33.33% extension in battery operational duration for wearable monitoring devices, assuming constant battery capacity and linear scaling of channel-related power consumption with channel count.

3.10. Comparative analysis of baseline and reduced configurations

To quantify the performance–efficiency tradeoff associated with channel reduction, a comprehensive comparative analysis was conducted between the baseline 16-channel and reduced 12-channel AdaBoost ensembles. Table 4 presents a side-by-side comparison of the key performance metrics across both configurations.

Table 4. Comparative performance analysis between the baseline 16-channel and reduced 12-channel AdaBoost ensembles

Metric	16-channel	12-channel	Difference
Training partition			
Accuracy (%)	99.96	99.93	−0.03
Sensitivity (%)	100.00	100.00	0.00
Specificity (%)	99.93	99.86	−0.07
Seizure miss rate (%)	0.00	0.00	0.00
Validation partition			
Accuracy (%)	99.11	99.00	−0.11
Sensitivity (%)	98.80	98.60	−0.20
Specificity (%)	99.50	99.50	0.00
Seizure miss rate (%)	1.20	1.40	+0.20
Testing partition			
Accuracy (%)	97.56	97.11	−0.45
Sensitivity (%)	97.29	96.71	−0.58
Specificity (%)	98.50	98.50	0.00
Seizure miss rate (%)	2.71	3.29	+0.58

To determine whether the observed performance differences between the baseline and reduced configurations were statistically significant, 95% Wilson score confidence intervals were computed for each metric, and two-proportion z-tests were conducted to compare the models. Table 5 presents the statistical comparison for the testing partition.

The comparative analysis revealed that the removal of four low-importance channels (x_5, x_9, x_{11}, and x_{13}) resulted in minimal degradation of classification performance. On the testing partition, which represents the most rigorous assessment of generalization capability, the reduced model exhibited an accuracy decrease of only 0.45 percentage points (from 97.56% to 97.11%) relative to the baseline configuration. This modest reduction suggests that the eliminated channels contributed limited additional

information to the model's classification performance.

Statistical analysis confirmed that the observed performance differences were not statistically significant. The two-proportion z-test for accuracy yielded $z = 0.585$ ($p = 0.558$), and the test for sensitivity yielded $z = 0.627$ ($p = 0.531$). The 95% confidence interval for the accuracy difference was −1.04% to +1.93%, and for the sensitivity difference was −1.22% to +2.36%. Both intervals include zero, indicating that the observed decreases of 0.45% in accuracy and 0.57% in sensitivity were not statistically distinguishable from random variation at the $\alpha = 0.05$ significance level. These findings support the conclusion that the 12-channel configuration achieved comparable classification performance to the baseline 16-channel model.

The sensitivity metric, which quantifies the model's ability to correctly identify seizure events, decreased by 0.58 percentage points on the testing set (from 97.29% to 96.71%). In absolute terms, this corresponded to an increase of four missed seizure detections, rising from 19 FNs in the baseline model to 23 FNs in the reduced model out of 700 total seizure events. Notably, specificity remained unchanged at 98.50% across both configurations, indicating that channel reduction did not adversely affect the model's capacity to correctly classify non-seizure episodes.

The seizure miss rate, a clinically relevant metric for ambulatory monitoring applications, increased from 2.71% to 3.29% following channel reduction. While this 0.58 percentage-point increase warrants consideration in clinical deployment decisions, it must be weighed against the substantial efficiency gains achieved through dimensionality reduction.

Figure 11 provides a visual comparison of the key performance metrics between the two configurations. The minimal height differences between paired bars indicate comparable classification performance following channel reduction.

Table 5. Statistical comparison of classification performance between the baseline 16-channel and the reduced 12-channel models on the testing partition

Metric	16-Channel (95% CI)	12-Channel (95% CI)	z-value	p-value
Accuracy (%)	97.56 (96.33–98.38)	97.11 (95.80–98.02)	0.585	0.558
Sensitivity (%)	97.29 (95.80–98.26)	96.71 (95.12–97.80)	0.627	0.531
Specificity (%)	98.50 (95.68–99.49)	98.50 (95.68–99.49)	0.000	1.000

Notes: CI was computed using the Wilson score method. z-values and p-values were obtained from two-proportion z-tests.
Abbreviation: CI: Confidence interval.

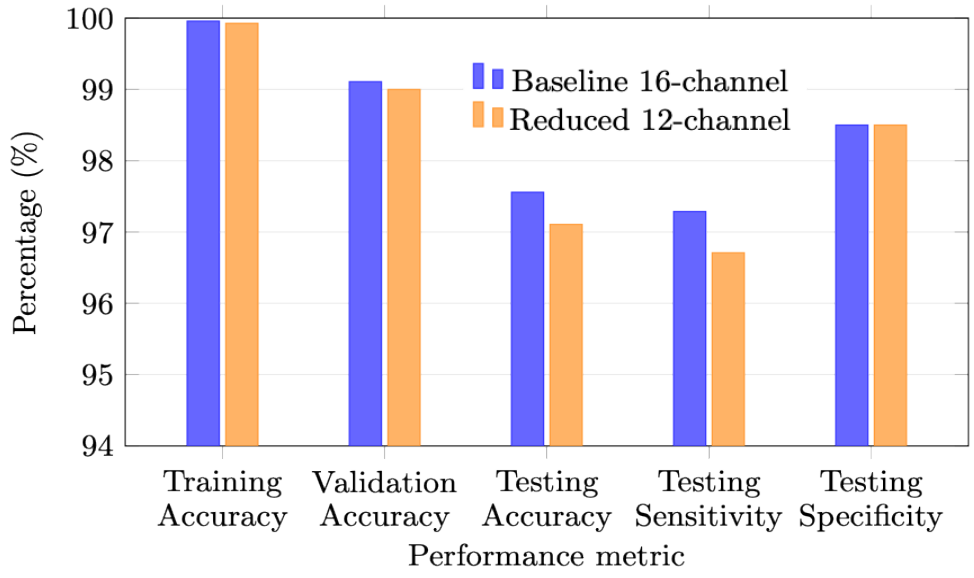

Figure 11. Comparative bar chart illustrating classification performance metrics for the baseline 16-channel and reduced 12-channel AdaBoost ensembles

From an efficiency perspective, the 25% reduction in active EEG channels translates directly to proportional decreases in analog-to-digital conversion operations, signal conditioning requirements, and feature extraction computations. According to the linear power consumption model, the reduced configuration is expected to consume approximately 75% of the power required by the baseline system. The corresponding 33.33% extension in theoretical battery life represents a potentially important improvement for wearable seizure detection devices intended for extended ambulatory monitoring periods.

The tradeoff analysis can be formalized by defining an efficiency-adjusted performance metric that balances classification accuracy against computational cost. Let η denote the efficiency gain ratio (equal to $16/12 = 1.333$ for the present comparison) and δ_A represent the fractional accuracy loss. The efficiency-adjusted score S is computed as:

$$S = \frac{A_{\text{reduced}}}{A_{\text{baseline}}} \times \eta = \frac{97.11}{97.56} \times 1.333 = 1.327 \quad (25)$$

A score exceeding unity indicates that the relative efficiency gain is greater than the relative reduction in accuracy, suggesting that the channel reduction represents a favorable tradeoff. The computed value of $S = 1.327$ confirms that the reduced 12-channel configuration provides a higher efficiency-to-performance ratio when both accuracy and computational efficiency are jointly considered.

In summary, the comparative analysis demonstrates that removing the four least important EEG channels resulted in a modest 0.45% decrease in test accuracy while achieving a 25% reduction in input channel dimensionality and an estimated 33.33% improvement in battery longevity. These findings support the viability of the reduced 12-channel configuration for resource-constrained wearable applications where extended operational duration is prioritized alongside acceptable classification performance.

4. Discussion

This study evaluated an optimized AdaBoost ensemble model for classifying epileptic and non-epileptic EEG signals using a reduced 12-channel configuration. By leveraging the inherent redundancy of multichannel EEG recordings, the model achieved a 33.33% theoretical increase in battery life with only a 0.45% accuracy reduction (p = 0.558), suggesting its potential suitability for long-term ambulatory monitoring.

4.1. Neurophysiological basis for channel reduction

Scalp EEG recordings exhibit substantial spatial correlation, as neighboring electrodes capture overlapping electrical activity.[21,22] Many automated systems underutilize these inter-channel relationships, focusing on individual electrodes rather than the topological structure of brain activity.[22] The present findings indicate that channel-level redundancy may be sufficient to permit reduction from 16 to 12 channels (removing x_5, x_9, x_{11}, and x_{13}) while maintaining stable classification performance, with the seizure miss rate increasing by only 0.58 percentage points.

Internal feature importance scores indicated that retained channels aligned with clinically relevant EEG markers.[25,26] Delta (<4 Hz) and theta (4–8 Hz) bands are established indicators of ictal activity in focal and generalized epilepsy[27,28], reflecting the transition from chaotic interictal states to hypersynchronous ictal activity.[28,29] Although our feature importance reflects channel-level rather than frequency-level contributions, the high accuracy suggests retained channels captured sufficient discriminative spectral information. Future frequency-domain explainability analyses may clarify specific signal characteristics driving classification.

4.2. Sources of classification errors

The slight increase in classification errors likely reflects two factors. First, high-frequency, low-amplitude fast activity characteristic of focal seizure onset[30,31] may become harder to distinguish from background noise with reduced spatial density.[32] Second, secondary generalized seizures originating focally before spreading rapidly[4,5,33] may be affected by spatial gaps in coverage. The BEED dataset adheres to the 10–20 system across frontal, temporal, parietal, occipital, and central regions[24], though explicit electrode-to-label mappings are unavailable. Channel removal necessarily reduces spatial sampling density in certain regions[34], potentially reducing sensitivity to seizure activity originating from areas represented by the removed channels.

Clinical acceptability of the observed 3.29% miss rate depends on intended use. For screening in low-risk populations, rates below 5% may be acceptable, whereas high-risk patients (e.g., those with sudden unexpected death in epilepsy risk) require stricter thresholds. This rate falls within ranges for ambulatory devices intended for seizure diary augmentation rather than critical alerting. Deployment decisions should weigh sensitivity against usability according to patient-specific risk profiles and intended clinical applications.

4.3. Clinical and hardware implications

The 33% theoretical battery life improvement enables multi-day monitoring beyond the "24-h barrier," addressing a primary bottleneck for patient compliance in ambulatory settings.[14,16,35] Channel count is among the strongest drivers of energy consumption in seizure detection devices; reduced maintenance frequency and device downtime further enhance clinical utility.[17,35] The simplified computational requirements make this AdaBoost ensemble potentially compatible with ultra-low-power architectures[17,36], enabling local processing without power-intensive continuous data streaming.[18]

We deliberately avoided direct performance comparisons with other published models because reported metrics cannot be reliably compared without documented convergence analysis confirming proper training dynamics. The learning curves in Figures 5 and 8 demonstrate stable convergence for our models. More fundamentally, demonstrating classifier superiority was not our objective; the central contribution is establishing channel reduction as a potential strategy for extending battery life without meaningful performance degradation. The statistically validated comparison between 16-channel and 12-channel configurations under identical conditions supports attribution of the observed performance changes primarily to channel reduction.

4.4. Methodological considerations

Generalizability was enhanced through patient-aware validation using a 70/15/15 split with complete patient separation between partitions, thereby reducing the risk of data leakage, which is a frequent pitfall where intra-patient similarities artificially inflate accuracy.[37,38] This "patient-independent" approach represents a rigorous evaluation strategy for clinical "cold start" scenarios.[39] AdaBoost's focus on hard-to-classify instances during training[19] likely contributed to the robust 97.11% accuracy.

The convergence of training and validation curves (gap ≈ 1 percentage point, stable throughout boosting iterations; Figures 5 and 8) indicates consistent learning behavior with limited evidence of overfitting, providing internal evidence of generalizability despite the absence of external validation on independent datasets.

4.5. Limitations and future directions

Several limitations warrant consideration. First, the BEED dataset does not provide explicit mappings between channel identifiers (x_1–x_{16}) and standard electrode names, thereby limiting precise neuroanatomical interpretation of channel removal effects. Second, power longevity benefits assume linear scaling with channel count; actual energy savings in wearable implementations depend on additional hardware-specific factors, including wireless transmission overhead, onboard memory operations, and processor architecture, in addition to temperature fluctuations.[14–16] Third, because feature importance rankings were derived from a single dataset, these rankings may not generalize to recordings obtained with different acquisition systems, electrode configurations, or patient populations; external validation across heterogeneous datasets is necessary to confirm the robustness of the proposed channel reduction strategy. Although external validation remains desirable, convergence analyses combined with patient-aware partitioning provide supportive evidence of model generalization within the evaluated dataset.

Future studies should validate the approach across demographically heterogeneous populations (pediatric, elderly)[40], test robustness in high-noise environments[41], and integrate the model into real-time clinical workflows connecting wearable devices with neurologist dashboards.[42,43] Despite limitations, the AdaBoost model's accuracy, generalizability, and power efficiency highlight its potential as a foundation for future ambulatory monitoring tools.[44]

5. Conclusion

This study demonstrates that the development of computationally efficient, ambulatory EEG systems does not necessarily require a compromise in diagnostic performance. By leveraging an optimized AdaBoost ensemble model and a strategic feature reduction approach, the input dimensionality was reduced from 16 channels to 12 channels. This modification led to a theoretically estimated 33% improvement in battery life, based on a linear power consumption model rather than experimental hardware measurements, while incurring only a 0.45% decrease in overall testing accuracy. These results suggest that the spatial redundancy in scalp EEG recordings can be effectively exploited to mitigate computational and energy constraints associated with medical-grade edge computing devices.

Furthermore, the robustness of these findings is supported by the patient-aware validation framework, which confirms that the observed performance was not attributable to patient-level data leakage within the evaluated dataset. While removal of four EEG channels may introduce minor localized spatial gaps, the model maintained high sensitivity (96.71%) and specificity (98.50%), supporting the feasibility of channel reduction for future long-term, out-of-hospital epilepsy management. By extending the theoretical operational window of these devices beyond the 24-h barrier, this research provides a

potential framework for improving the energy efficiency of autonomous seizure detection systems. This approach may contribute toward the development of practical ambulatory monitoring solutions that enhance patient compliance and provide clinicians with continuous, real-world data from their patients.

Acknowledgments

None.

Funding

The authors declare that no external financial support or grants were received from any funding agency or commercial organization to perform the research, analysis, or publication of this article. This work was supported solely by institutional resources provided by the authors' affiliated institutions.

Conflict of interest

The authors declare they have no competing interests.

Author contributions

Conceptualization: All authors
Formal analysis: All authors
Investigation: All authors
Methodology: All authors
Writing–original draft: All authors
Writing–review & editing: All authors

Ethics approval and consent to participate

Not applicable.

Consent for publication

Not applicable.

Availability of data

Not applicable.

Further disclosure

The authors declare that no generative artificial intelligence tools were used in the conception, design, data collection, analysis, interpretation of results, or generation of any text, figures, or tables in this manuscript. All intellectual content represents the original work of the authors. During manuscript preparation, grammar and spelling verification software (Grammarly) was used for proofreading purposes. The authors acknowledge that such tools may incorporate artificial intelligence-based components for grammar checking; however, these were used solely for surface-level language corrections and did not contribute to the generation of any substantive content. The authors take full responsibility for the accuracy, integrity, and originality of the entire manuscript.

References

1. World Health Organization. *Epilepsy: A Public Health Imperative*. World Health Organization; 2019. https://iris.who.int/handle/10665/325293
2. World Health Organization. Epilepsy. World Health Organization; 2024. https://www.who.int/news-room/fact-sheets/detail/epilepsy
3. Institute for Quality and Efficiency in Health Care (IQWiG). Overview: Epilepsy. In: *InformedHealth.org [Internet]*. Institute for Quality and Efficiency in Health Care (IQWiG); 2023. https://www.ncbi.nlm.nih.gov/books/NBK343313/
4. McWilliam M, Asuncion RMD, Al Khalili Y. Idiopathic (genetic) generalized epilepsy. In: *StatPearls [Internet]*. StatPearls Publishing; 2024. https://www.ncbi.nlm.nih.gov/books/NBK546611/
5. Beniczky S, Trinka E, Wirrell E, *et al*. A practical guide to the updated seizure classification 2025. *Epileptic Disord*. 2025;27(6):1087-1104.

   doi: 10.1002/epd2.70110
6. Benbadis SR, Beniczky S, Bertram E, MacIver S, Moshé SL. The role of EEG in patients with suspected epilepsy. *Epileptic Disord*. 2020;22(2):143-155.

   doi: 10.1684/epd.2020.1151
7. Seneviratne U, Cook M, D'Souza W. Brainwaves beyond diagnosis: Wider applications of electroencephalography in idiopathic generalized epilepsy. *Epilepsia*. 2021;63(1):22-41.

   doi: 10.1111/epi.17119
8. Schulze-Bonhage A, Bruno E, Brandt A, *et al*. Diagnostic yield and limitations of in-hospital documentation in patients with epilepsy. *Epilepsia*. 2022;64(S4).

   doi: 10.1111/epi.17307
9. Tatum WO, Mani J, Jin K, *et al*. Minimum standards for inpatient long-term video-eeg monitoring: A clinical practice guideline of the international league against epilepsy and international federation of clinical neurophysiology. *Clin Neurophysiol*. 2022;134:111-128.

   doi: 10.1016/j.clinph.2021.07.016
10. Ambulatory EEG. In: *Handbook of Clinical Neurology*. Elsevier; 2019:161-170.

    doi: 10.1016/b978-0-444-64032-1.00010-2
11. Hadady L, Robinson T, Bruno E, Richardson MP, Beniczky S. Users' perspectives and preferences on using wearables in epilepsy: A critical review. *Epilepsia*. 2025;66(S3):4-13.

    doi: 10.1111/epi.18280

12. Saifutdinova E, Congedo M, Dudysova D, Lhotska L, Koprivova J, Gerla V. An Unsupervised Multichannel Artifact Detection Method for Sleep EEG Based on Riemannian Geometry. *Sensors*. 2019;19(3):602.

doi: 10.3390/s19030602

13. Frankel MA, Lehmkuhle MJ, Spitz MC, Newman BJ, Richards SV, Arain AM. Wearable Reduced-Channel EEG System for Remote Seizure Monitoring. *Front Neurol*. 2021;12.

doi: 10.3389/fneur.2021.728484

14. Casson A, Yates D, Smith S, Duncan J, Rodriguez-Villegas E. Wearable Electroencephalography. *IEEE Eng Med Biol Mag*. 2010;29(3):44-56.

doi: 10.1109/memb.2010.936545

15. Tian F, Yang J, Zhao S, Sawan M. NeuroCARE: A generic neuromorphic edge computing framework for healthcare applications. *Front Neurosci*. 2023;17.

doi: 10.3389/fnins.2023.1093865

16. Covi E, Donati L, Liang X, *et al*. Adaptive extreme edge computing for wearable devices. *Front Neurosci*. 2021;15.

doi: 10.3389/fnins.2021.611300

17. Reisinger P, Larochelle J, Abkai C, *et al*. The impact of EEG preprocessing parameters on ultra-low-power seizure detection. *Epilepsia*. 2025;66(10):3895-3906.

doi: 10.1111/epi.18521

18. Zendehbad SA, Razavi AS, Tabrizi N, Sedaghat Z. A systematic review of artificial intelligence techniques based on electroencephalography analysis in the diagnosis of epilepsy disorders: A clinical perspective. *Epilepsy Res*. 2025;215:107582.

doi: 10.1016/j.eplepsyres.2025.107582

19. Schapire RE, Singer Y. Improved Boosting Algorithms Using Confidence-rated Predictions. *Mach Learn*. 1999;37(3):297-336.

doi: 10.1023/a:1007614523901

20. Ding Y, Zhu H, Chen R, Li R. An Efficient AdaBoost Algorithm with the Multiple Thresholds Classification. *Appl Sci*. 2022;12(12):5872.

doi: 10.3390/app12125872

21. Ekpar FE, Njoku FA. Analysis of electroencephalography (EEG) electrode-pair correlations. *EJECE*. 2023;7(6):6-10.

doi: 10.24018/ejece.2023.7.6.571

22. Xu Z, Ge H, Huang W, Lu H. Epilepsy detection based on spatiotemporal feature interaction fusion of EEG signals. *Front Neurol*. 2026;16.

doi: 10.3389/fneur.2025.1478718

23. Kerr WT, McFarlane KN, Figueiredo Pucci G. The present and future of seizure detection, prediction, and forecasting with machine learning, including the future impact on clinical trials. *Front Neurol*. 2024;15.

doi: 10.3389/fneur.2024.1425490

24. Rajput V. BEED: Bangalore EEG epilepsy dataset. Kaggle; 2025. https://www.kaggle.com/datasets/varunrajput/beed-bangalore-eeg-epilepsy-dataset

25. Farooq MS, Zulfiqar A, Riaz S. Epileptic seizure detection using machine learning: Taxonomy, opportunities, and challenges. *Diagnostics*. 2023;13(6):1058.

doi: 10.3390/diagnostics13061058

26. Sun Y, Ren G, Ren J, Wang Q. High-frequency oscillations detected by electroencephalography as biomarkers to evaluate treatment outcome, mirror pathological severity and predict susceptibility to epilepsy. *Acta Epileptol*. 2021;3(1).

doi: 10.1186/s42494-021-00063-z

27. Segovia-Oropeza M, Rauf EHU, Heide E, Focke NK. Quantitative EEG signatures in patients with and without epilepsy development after a first seizure. *Epilepsia Open*. 2025;10(2):427-440.

doi: 10.1002/epi4.13128

28. Fisher RS, Scharfman HE, deCurtis M. How Can We Identify Ictal and Interictal Abnormal Activity? In: *Advances in Experimental Medicine and Biology*. Springer Netherlands; 2014:3-23.

doi: 10.1007/978-94-017-8914-1_1

29. Wendling F, Hernandez A, Bellanger JJ, Chauvel P, Bartolomei F. Interictal to ictal transition in human temporal lobe epilepsy: Insights from a computational model of intracerebral EEG. *J Clin Neurophysiol*. 2005;22(5):343-356.

30. Worrell G. High-Frequency Oscillations Recorded on Scalp EEG. *Epilepsy Curr*. 2012;12(2):57-58.

doi: 10.5698/1535-7511-12.2.57

31. Arroyo S, Uematsu S. High-Frequency EEG Activity at the Start of Seizures. *J Clin Neurophysiol*. 1992;9(3):441-448.

doi: 10.1097/00004691-199207010-00012

32. Asayesh A, Vanhatalo S, Tokariev A. The impact of EEG electrode density on the mapping of cortical activity networks in infants. *NeuroImage*. 2024;303:120932.

doi: 10.1016/j.neuroimage.2024.120932

33. National Institute of Neurological Disorders and Stroke. Epilepsy and seizures. 2026. https://www.ninds.nih.gov/health-information/disorders/epilepsy-and-seizures

34. Acharya JN, Hani A, Cheek J, Thirumala P, Tsuchida TN. American Clinical Neurophysiology Society Guideline 2: Guidelines for Standard Electrode Position Nomenclature. *J Clin Neurophysiol*. 2016;33(4):308-311.

doi: 10.1097/wnp.0000000000000316

35. Fabian D, Ahmed I. Ambulatory ECG Monitoring. In: *StatPearls [Internet]*. StatPearls Publishing; 2026. https://www.ncbi.nlm.nih.gov/books/NBK597374/

36. Al-Hadeethi H, Abdulla S, Diykh M, Green JH. Determinant of Covariance Matrix Model Coupled with AdaBoost Classification Algorithm for EEG Seizure Detection. *Diagnostics*. 2021;12(1):74.

doi: 10.3390/diagnostics12010074

37. Brookshire G, Kasper J, Blauch NM, *et al*. Data leakage in deep learning studies of translational EEG. *Front Neurosci*. 2024;18.

doi: 10.3389/fnins.2024.1373515

38. Starcke J, Spadafora J, Spadafora J, Spadafora P, Toma M. The Effect of Data Leakage and Feature Selection on Machine Learning Performance for Early Parkinson's Disease Detection. *Bioengineering*. 2025;12(8):845.

doi: 10.3390/bioengineering12080845

39. Abou-Abbas L, Henni K, Jemal I, Mitiche A, Mezghani N. Patient-independent epileptic seizure detection by stable feature selection. *Expert Syst Appl*. 2023;232:120585.

doi: 10.1016/j.eswa.2023.120585

40. Yu J, Zhang L, Cheng D, *et al*. Ensemble early exit network on human activity recognition using wearable sensors. *Comput Netw*. 2025;269:111409.

doi: 10.1016/j.comnet.2025.111409

41. Ferree TC, Luu P, Russell GS, Tucker DM. Scalp electrode impedance, infection risk, and EEG data quality. *Clin Neurophysiol*. 2001;112(3):536-544.

doi: 10.1016/s1388-2457(00)00533-2

42. Zhang R, Sui L, Gong J, Cao J. EEG-based real-time diagnostic system with developed dynamic 2TEMD and dynamic ApEn algorithms. *Front Physiol*. 2023;14.

doi: 10.3389/fphys.2023.1165450

43. Nasef D, Nasef D, Sawiris V, Weinstein B, Garcia J, Toma M. Integrating artificial intelligence in clinical practice, hospital management, and health policy: literature review. *J Hosp Manag Health Policy*. 2025;9:20-20.

doi: 10.21037/jhmhp-24-138

44. Siddiqui MIH, Sakib AH, Akter S, Debnath J, Mahmud MR. Comparative analysis of traditional machine learning vs deep learning for sleep stage classification. *Int J Sci Res Arch*. 2025;15(1):1778-1789.

doi: 10.30574/ijsra.2025.15.1.1159